STATUS ON DEVELOPMENT AND VERIFICATION OF REACTIVITY INITIATED ACCIDENT ANALYSIS CODE FOR PWR (NODAL3)

Peng Hong Liem [1], Surian Pinem [2], Tagor Malem Sembiring [2]
and Tran Hoai Nam [3]

[1] *Nippon Advanced Information Service (NAIS Co., Inc.)*
416 Muramatsu, Tokaimura, Ibaraki 319-1112, Japan
e-mail: liemph@nais.ne.jp

[2] *National Nuclear Energy Agency of Indonesia (BATAN),*
Kawasan Puspiptek Gd. No. 80 Serpong, Tangerang Selatan 15310, Indonesia
e-mail: pinem@batan.go.id
e-mail: tagorms@batan.go.id

[3] *Institute of Research and Development, Duy Tan University,*
K7/25 Quang Trung, Da Nang, Vietnam
e-mail: tranhoainam4@dtu.edu.vn

Abstract: A coupled neutronics thermal-hydraulics code NODAL3 has been developed based on the nodal few-group neutron diffusion theory in 3-dimensional Cartesian geometry for a typical pressurized water reactor (PWR) static and transient analyses, especially for reactivity initiated accidents (RIA). The spatial variables are treated by using a polynomial nodal method (PNM) while for the neutron dynamic solver the adiabatic and improved quasi-static methods are adopted. A simple single channel thermal-hydraulics module and its steam table is implemented into the code. Verification works on static and transient benchmarks are being conducting to assess the accuracy of the code. For the static benchmark verification, the IAEA-2D, IAEA-3D, BIBLIS and KOEBERG light water reactor (LWR) benchmark problems were selected, while for the transient benchmark verification, the OECD NEACRP 3-D LWR Core Transient Benchmark and NEA-NSC 3-D/1-D PWR Core Transient Benchmark (Uncontrolled Withdrawal of Control Rods at Zero Power). Excellent agreement of the NODAL3 results with the reference solutions and other validated nodal codes was confirmed.

Keywords: coupled neutronics thermal-hydraulics, nodal method, adiabatic method, improved quasi-static method, PWR, reactivity initiated accident, benchmark verification

I. INTRODUCTION

The National Nuclear Energy Agency of Indonesia (BATAN) has been operating three research reactors with the nominal thermal power of 100 kW, 2 MW and 30 MW, respectively, for nuclear science, technology and engineering research and development (R&D) as well as for training and education in the Agency and universities. The oldest 100 kW reactor has been operated safely since back to 1965. The introduction of nuclear power plant (NPP) was several times delayed due to the strong dependency of the national primary energy on the fossil fuels [1]. However, recently, the evaluation of NPP reactor safety is becoming an important R&D activities in the Agency since the nuclear option has been included into the policy of the national energy mix up to the fiscal year of 2025 [2]. One of the highly prioritized R&D activities in BATAN as a Technical Support Organization (TSO) presently is to build the

capability for developing analytical tools for in-core fuel management and transient analysis of typical NPPs, especially pressurized water reactors (PWRs).

The development of analytical tools in the Agency was initiated back to 2 decades ago by the development of standardized 2-dimensional (2-D) and 3-dimensional (3-D) multigroup neutron diffusion codes for various types of research reactors, namely the BATAN-2DIFF and BATAN-3DIFF codes, respectively [3-6]. There are several special features of those codes do not exist in other similar generic codes, such as the capability of estimating the radial and axial power peaking factors based on the mesh-averaged and mesh-edge approaches for each core-grid or fuel element position. Satisfactory results of verification and validation of the codes have been confirmed through several calculation benchmarks as well as against the experimental results using a critical assembly and a research reactor [7-11]. Furthermore, an in-core fuel management code for research reactors has been developed based on those computer modules [12, 13]. The in-core fuel management code, BATAN-FUEL, has been used for establishing the new equilibrium core of the 30 MWth RSG GAS multipurpose reactor using silicide fuel with higher uranium fuel loading. Currently the code is being used for routine in-core fuel management of RSG GAS reactor [14, 15]. The BATAN-FUEL code has also several unique features such as the capability to search automatically an equilibrium core without performing lengthy and time consuming transient cores.

In the last several years, a 3-D coupled neutronics and thermal-hydraulic calculation code, MTR-DYN, had been developed for safety analysis of a material testing research reactor (MTR) [16] such as the RSG GAS. Several transient characteristics of the RSG GAS reactor, e.g. reactivity initiated accident (RIA), reduced primary coolant flow rate, and some combination of abnormal event scenarios had been analyzed by using the MTR-DYN code [16, 17].

Based on the experiences in developing the static and transient calculation codes for research reactors, the development of the in-core fuel management and 3-D transient analysis codes is extended to typical PWRs. PWR-type reactor has been selected based on the guidance of the national research programs [18]. These research programs are expected to assist the design evaluation of several PWR candidates which are expected to be offered and introduced by several international vendors.

It is well-known that the PWR core dimension is considerably much larger compared to one of a research reactor, so that the neutron diffusion problem in a PWR is commonly solved by modern nodal methods [19]. Therefore, besides the finite-difference method adopted in the BATAN-2DIFF, BATAN-3DIFF, BATAN-FUEL and MTR-DYN codes, a nodal method has to be introduced for the spatial treatment. The nodal method adopted here is based on the polynomial nodal method (PNM) proposed by Finnemann et al. [20]. The NODAL3 code, developed in this study, solves steady-state as well as time-dependent few-group neutron diffusion equations in 3-D Cartesian geometry and coupled with a simple thermal-hydraulic model for a typical PWR.

The NODAL3 code has been verified with the steady state light water reactor (LWR) benchmarks, such as IAEA-2D, IAEA-3D, KOERBERG, and BIBLIS light water reactors, and very satisfactory results were obtained [21]. The code is presently also being verified for

transient LWR benchmarks. The transient benchmark verification works cover the well-known NEACRP 3-D LWR Core Transient Benchmark [22] and PWR Benchmark on Uncontrolled Rods Withdrawal at Zero Power [23]. The two benchmarks represent a severe reactivity initiated accident (RIA) due to single or multiple control rod ejection which is one important challenge to PWR safety. The benchmarks were selected since many organizations participated using various methods as well as approximations [22], so that in addition to the reference solutions, the calculation results of NODAL3 code can also be compared to other codes' results.

This paper reports some of the benchmark calculation results of NODAL3 code for static and transient cases. In Section II, the NODAL3 code is briefly explained, especially on the kinetic models adopted. Sections III and IV elaborate the benchmark calculation results for static and transient cases, respectively. The last section, Section V gives the conclusions and future works.

II. NODAL3 BRIEF DESCRIPTION

NODAL3 code consists of three modules; the first module deals with the nodal equation for the steady state problems; the second module deals with the thermal-hydraulics model of a typical PWR fuel pin (static and time-dependent single channel analytical model); and the third module is the time-dependent solver for the reactor dynamics. In the first module, the few-group neutron diffusion equation in 3-D Cartesian geometry is discretized spatially using the polynomial nodal method (PNM). A coarse mesh finite difference (CFMD) formulation is used to determine the node-averaged neutron fluxes and the eigenvalue, while the PNM method is used to estimate the accurate coupling between adjacent nodes in the core. Quadratic polynomial expansion for the transverse-integrated flux is adopted [24]. The detail description the PNM implementation in the NODAL3 code can be found in Refs. [21, 25].

In the second module, i.e. the thermal-hydraulic module, the heat conduction problem in the fuel rods is discretized in time and space using the conventional finite-difference method. Heat conduction is considered only in the radial direction. Fluid dynamic of the cooling water is modeled under a single-phase flow condition. The mass flow rate in each cooling channel is assumed to be known and specified by the code user. As a result, only the mass continuity and energy conservation equations are to be solved. These are discretized in space and time using finite-difference method and implicit scheme, respectively [25]. An appropriate steam table covering the operational temperature and pressure of PWR and BWR is included in the NODAL3 code [25]. The thermal-hydraulics calculations in term of fuel temperature, moderator (coolant) temperature and density are fed back via appropriate macroscopic cross-sections.

In the third module, two time-dependent reactor dynamics models are available, i.e. the adiabatic method (AM) and improved quasistatic methods (IQSM). These two methods are selected since they have a high accuracy [25]. This section describes briefly the application of these methods. The spatial and time-dependent group neutron flux is assumed can be factorized into [26]:

$$\phi_g(r,t) = p(t)\Psi_g(r,t), \quad p(0) = 1 \tag{1}$$

where $p(t)$ and $\Psi_g(r,t)$ are the time-dependent amplitude and shape functions, respectively. Under this assumption, the time-dependent few-energy group neutron diffusion equation is commonly written as follows.

$$\begin{aligned}\frac{1}{v_g}\cdot\left(\frac{\partial\Psi_g(r,t)}{\partial t}+\frac{1}{p(t)}\cdot\frac{dp(t)}{dt}\Psi_g(r,t)\right) &= \nabla D_g(r,t)\cdot\nabla\Psi_g(r,t)-\Sigma_{rg}(r,t)\Psi_g(r,t)\\ &+\sum_{g'=1}^{G}\Sigma_{sg'\to g}(r,t)\Psi_{g'}(r,t)\\ &+\chi_{pg}\sum_{g'=1}^{G}\nu_{pg'}\Sigma_{fg'}(r,t)\Psi_{g'}(r,t)\\ &+\frac{1}{p(t)}\sum_{k=1}^{K}\chi_{dkg}\lambda_k C_k(r,t),\\ g&=1,\cdots,G\\ k&=1,\ldots,K\end{aligned}\qquad(2)$$

where:

g - prompt neutron energy group index;
G - total number of prompt neutron energy groups;
k - delayed neutron energy group index;
K - total number of delayed neutron energy groups;
p - prompt neutron index;
d - delayed neutron index;
v_g - neutron speed [cm s^{-1}];
$\Psi_g(r,t)$ - time-dependent shape function [cm^{-2} s^{-1}];
$p(t)$ - time-dependent amplitude function;
$D_g(r,t)$ - diffusion coefficient in time t [cm];
$\Sigma_{rg}(r,t)$ - macroscopic removal cross section in time t [cm^{-1}];
$\Sigma_{sg'\to g}(r,t)$ - macroscopic scattering cross section from group g' to g in time t [cm^{-1}];
$\nu_{pg'}\Sigma_{fg'}(r,t)$ - number of prompt neutrons emitted per fission times macroscopic fission cross section in time t [cm^{-1}];
χ_{pg} - fission spectrum of prompt neutron;
χ_{dkg} - fission spectrum of delayed neutron;
λ_k - decay constant of precursors [s^{-1}];
$C_k(r,t)$ - concentration of delayed neutron precursors in time t [cm^{-3}];

In the AM, firstly, the difference between the neutron spectra of delayed neutrons and the ones of prompt neutrons are neglected. In other words, the delayed neutrons from their precursors are assumed to be born at the same time with the prompt neutrons. Secondly, all

time derivatives of the amplitude and shape functions are neglected. Thus, Eq. (1) is simplified as:

$$\nabla D_g(r,t)\cdot\nabla\Psi_g(r,t)-\Sigma_{rg}(r,t)\Psi_g(r,t)+\sum_{g'=1}^{G}\Sigma_{sg'\to g}(r,t)\Psi_{g'}(r,t)$$
$$+\frac{1}{k_{eff}}\chi_g\sum_{g'=1}^{G}\nu_{g'}\Sigma_{fg'}(r,t)\Psi_{g'}(r,t)=0 \tag{3}$$

where k_{eff} in Eq. (3) is the effective multiplication factor after the perturbation occurred. The usual eigenvalue criticality procedure can be readily applied to solve the shape function. The obtained $\Psi_g(r,t)$ again is used to calculate the new cross sections and other parameters.

In the IQSM, the time derivative of the shape function is approximated with the backward finite difference scheme,

$$\frac{\partial\Psi_g(r,t)}{\partial t}\to\frac{\Psi_g(r,t)-\Psi_g(r,t-\Delta t_s)}{\Delta t_s} \tag{4}$$

so that Eq. (1) is approximated as follows:

$$\frac{1}{v_g}\cdot\left(\frac{\Psi_g(r,t)}{\Delta t_s}+\frac{1}{p(t)}\cdot\frac{dp(t)}{dt}\Psi_g(r,t)\right)=\nabla D_g(r,t)\cdot\nabla\Psi_g(r,t)-\Sigma_{rg}(r,t)\Psi_g(r,t)$$
$$+\sum_{g'=1}^{G}\Sigma_{sg'\to g}(r,t)\Psi_{g'}(r,t)$$
$$+\chi_{pg}\sum_{g'=1}^{G}\nu_{pg'}\Sigma_{fg'}(r,t)\Psi_{g'}(r,t)$$
$$+\frac{1}{p(t)}\sum_{k=1}^{K}\chi_{dkg}\lambda_k C_k(r,t) \tag{5}$$
$$+\frac{\Psi_g(r,t-\Delta t_s)}{v_g\Delta t_s}$$
$$g=1,\cdots,G.$$

Obviously IQSM is expected to give the better accuracy than AM. For both methods, the most time consuming part is the shape function calculations.

In addition to the three modules, which is not less important is the time-step adjustment. Different time steps for amplitude function (Δt_a), shape function (Δt_s), and thermal-hydraulic calculation (Δt_t) are adopted in NODAL3 code in order to obtain accurate results with minimal computation times. In some cases, another time step for reactivity calculation (Δt_ρ) is required for simulating the movement of the control rod. There is no definitive rule to determine the optimal time steps and best relations among them. However, we usually adopt the following

rule [25] to determine them manually. The Δt_a should be taken small enough to maintain the accuracy and stability since the stability of the amplitude function is a necessary condition for the stability of other part of the calculations. In NODAL3 code, the amplitude function is solved using a fourth order explicit Runge-Kutta method with a typical time step in the order of 1.0×10^{-5} seconds. On the other hand, Δt_s and Δt_ρ are determined through observation of the shape function transient rate. In the practical use of the AM, the temperature change gives a relatively smaller effect on the shape function compared to the composition change, such as a rod withdrawal. Thus, while composition changes occur, smaller Δt_s and Δt_ρ should be adopted. However, the existence of the solutions of the criticality problem in Eq. (3) is independent from Δt_s. During the time intervals, where no composition change occurs, Δt_ρ should not be taken less than Δt_s or Δt_t, and shape function calculation should wait until thermal-hydraulics calculation is done. The Δt_t is strongly dependent on the accumulation rate of energy (time integrated reactor power) or the transient rate of amplitude function. When the temperature increase/decrease produces no significant change in the reactivity, thermal-hydraulics calculation can be delayed until needed. Of course, Δt_t has to be checked to preserve the stability of the thermal-hydraulics calculation itself. NODAL3 code is also equipped with an automatic algorithm for time step adjustment based on the rule and users are recommended to use the option.

III. STATIC BENCHMARK CALCULATION RESULTS

Although the ultimate purpose of the NODAL3 code development is for PWR RIA analyses, the accuracy of the steady-state (static) analysis results should also be verified since the results will be used for the initial conditions of transient analyses. We have selected the following static benchmark problems: IAEA-2D, BIBLIS and KOEBERG LWRs for 2-D geometry [27], and IAEA-3D for 3-D geometry [28]. The benchmark specifications and reference solutions are well documented in Refs. [27, 28] and readers should consult the references. Besides the effective multiplication factor (k_{eff}), the radial and axial (3-D) power distributions were also evaluated.

Table 1. Benchmark calculation results of NODAL3 for 2-D LWR geometry (k_{eff}).

Benchmark Problem	Fuel Element Pitch (cm)	NODAL3		k_{eff} Ref. Solution [27]	Deviation (Δk_{eff}(%))
		No of Node	k_{eff}		
IAEA-2D	20	1 × 1	1.029441	1.029585	0.014
		2 × 2	1.029528		0.006
BIBLIS-2D	23.1226	1 × 1	1.025202	1.025110	0.009
		2 × 2	1.025095		0.001
KOEBERG	21.608	1 × 1	1.008392	1.007954	0.044
		2 × 2	1.008002		0.005

Benchmark calculation results (k_{eff} and radial power distribution) of NODAL3 for 2-D reactor geometry are shown in Tables 1 and 2. From Table 1, if one fuel assembly (FA) is represented by a single node the maximum deviation of k_{eff} is less than 0.044%. For 2 × 2 nodes cases, higher accuracy is obtained and the maximum deviation of k_{eff} can be minimized to 0.006%. The deviation of IAEA-2D is relatively larger than other cases. This is attributed to the

existence of large neutron flux gradient due to control rods. From Table 2, one can also observe a good agreement of the radial power distributions of NODAL3 with the reference solutions. Increasing the number of node per FA also improves the accuracy of the power distributions.

Table 2. Benchmark calculation results of NODAL 3 for 2-D LWR geometry (radial power distribution).

Benchmark Problem	NODAL3		FPD_{Rmax} Ref. Solution [27]	Deviation of FPD_{Rmax} (Ref - NODAL3)	RMS (root mean square)
	No of Node per FA	FPD_{Rmax}			
IAEA-2D	1 × 1	1.496	1.480	-0.016	1.0654×10^{-2}
	2 × 2	1.486		0.006	4.1997×10^{-3}
BIBLIS-2D	1 × 1	1.245	1.243	-0.002	5.2859×10^{-3}
	2 × 2	1.245		-0.002	1.7652×10^{-3}
KOEBERG	1 × 1	1.233	1.243	0.010	1.3451×10^{-2}
	2 × 2	1.242		0.001	1.2453×10^{-3}

Note: FPD_R and FPD_{Rmax} denote radial power peaking factor and its maximum value.

Benchmark calculations results of NODAL3 for 3-D reactor geometry are shown in Tables 3 and 4 for k_{eff} values. From Table 3, one can observe that increasing the number of node per FA minimizes the k_{eff} deviation significantly. In Table 4, we compare the k_{eff} and its deviation of NODAL3 with other validated nodal codes such as PARCS [29] and NESTLE [30]. The accuracy of NODAL3 is the same or higher than those codes.

Table 3. Benchmark calculation results of NODAL3 for 3-D LWR geometry (k_{eff}).

Benchmark Problem	FA Pitch (cm)	NODAL3			k_{eff} Ref. Solution [28]	Deviation (Δk_{eff}(%))
		No of Radial Node per FA	No of Axial Node	k_{eff}		
IAEA-3D	20	1 × 1	17	1.02892	1.02904	0.012
		2 × 2	17	1.02900		0.004

Table 4. Comparison of NODAL3 benchmark result with other validated nodal codes (k_{eff}).

Nodal Code	k_{eff}	k_{eff} Ref. Solution [28]	Deviation (Δk_{eff}(%))
NODAL3 *)	1.02900	1.02904	0.004
PARCS	1.02910		0.006
NESTLE	1.02909		0.005

*) No of radial (per FA) and axial (per layer) nodes are 2 × 2 and 17, respectively.

Tables 5 and 6 show the benchmark calculation results of NODAL3 for radial power distribution. As in the 2-D reactor geometry cases, good agreement with the reference solution is confirmed. Comparison result with other nodal codes also indicates the high accuracy of NODAL3 code in predicting the radial power peaking factors. Table 7 summarizes the comparison of NODAL3 radial power distribution result with reference solution and other nodal codes. Compared to other validated nodal codes, the same degree of accuracy is confirmed.

Table 5. Benchmark calculation results of NODAL3 for 3-D LWR geometry (radial power distribution).

Benchmark Problem	NODAL3		FPD_{Rmax} Ref. Solution [28]	Deviation of FPD_{max} (Ref. – NODAL3)	RMS (root mean square)
	No of Radial Node per FA	FPD_{Rmax}			
IAEA-3D	1 × 1	1.443	1.432	-0.011	7.1683×10^{-3}
	2 × 2	1.433		-0.001	1.0919×10^{-3}

Table 6. Comparison of NODAL3 benchmark result with other validated nodal codes (radial power distribution).

Nodal Code	FPD_{Rmax}	FPD_{Rmax} Ref. Solution [28]	Deviation of FPD_{Rmax} (Ref. – Code)	RMS (root mean square)
NODAL3[*)]	1.433	1.432	-0.001	1.0919×10^{-3}
PARCS	1.425		0.007	5.0203×10^{-3}
NESTLE	1.426		0.006	4.2088×10^{-3}

[*)] No of radial (per FA) and axial nodes are 2 × 2 and 17, respectively.

Table 7. Comparison of NODAL3 benchmark result with reference solution and other validated nodal codes (axial power distribution).

Nodal Code	FPD_{Amax}	FPD_{Amax} Ref. Solution [28]	Deviation of FPD_{Amax} (Ref. – Code)
NODAL3 (1 × 1)	1.557	1.607	0.050
NODAL3 (2 × 2)	1.556		0.051
PARCS	1.553		0.054
NESTLE	1.555		0.052

Note: FPD_A and FPD_{Amax} denote axial power peaking factor and its maximum value.

IV. TRANSIENT BENCHMARK CALCULATION RESULTS

For the transient benchmark problems, the NEACRP 3-D LWR Core Transient Benchmark [22] and PWR Benchmark on Uncontrolled Rods Withdrawal at Zero Power [23] were selected. The specifications of the benchmark problems are given in Refs. [22, 23] and readers should consult the references. Control rod ejection events, stipulated in the benchmarks, may occur as a consequence of the rupture of the control rod drive mechanism (CRDM) in a PWR. This event is followed by a significant localized fast perturbation of the neutronics and thermal-hydraulics core parameters which challenges the accuracy of any nodal code.

In this paper we only report some results [31] for the NEACRP 3-D LWR Core Transient Benchmark. The transient events in the benchmark are initiated by a rapid ejection of control rod (CR) at HZP (hot zero power, 2775 W) and HFP (hot full power, 2775 MW) conditions. The core configuration and operational data, such as geometry and neutron cross sections, are derived from a real PWR. To allow the problem of a single rod ejection, a CR is added in the center of the core. As shown in Ref. [22], there are 6 cases in the benchmark, i.e. Case A, B and C for both HZP and HFP conditions. In this work, only 4 cases are selected, namely Case A and B (HZP and HFP), since the initial all control rod positions in the problem Case C (HFP) are quite similar to the Case A and Case B (HFP), although the position of the ejected CR in Cases A or B and Case C are not same. The four selected cases are described in Table 8 and Fig. 1. In

this work, the benchmark cores are modeled in a symmetrical quarter core geometry with 2 × 2 nodes for a FA in radial direction, and 1 (one) node for each layer axially. Some mandatory assumptions in thermal-hydraulic method are made in the benchmark specification, such as fuel conductance which is constant and rod expansion and cross flow effects are not considered. Therefore, the thermal relations and properties in the NODAL3 code, such as heat conductivity and specific heat capacity were identical with the thermal relations of the benchmark data.

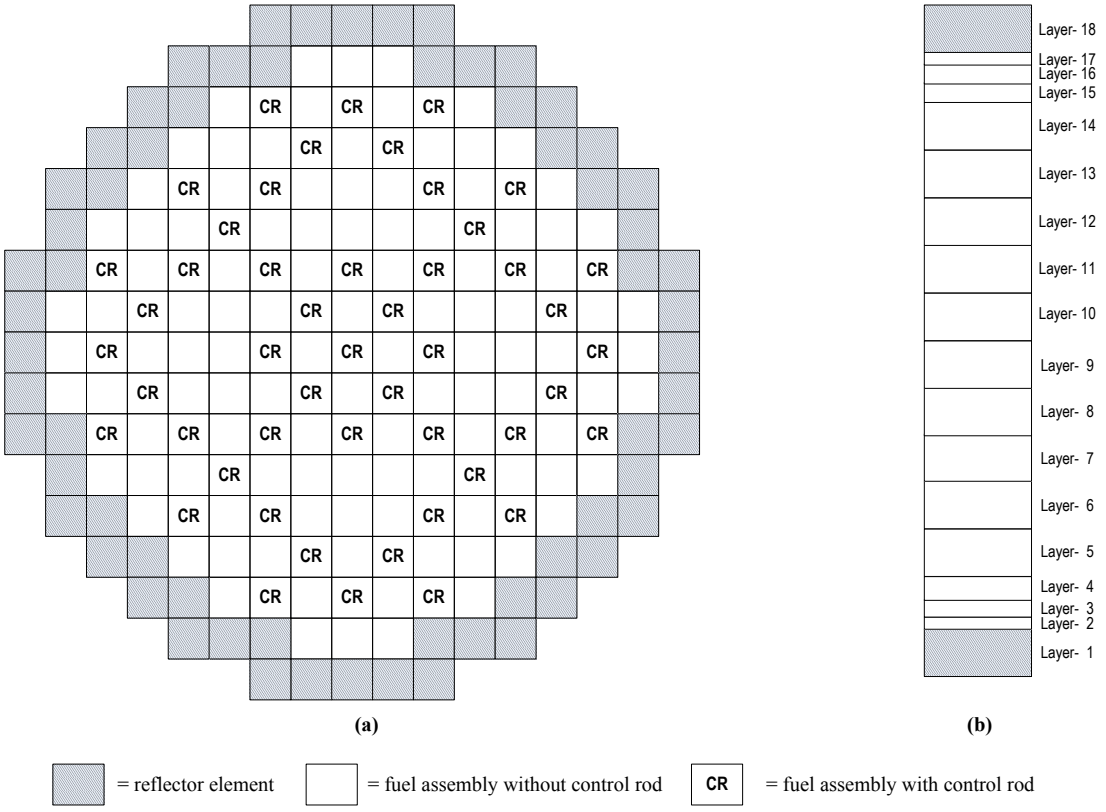

Figure 1. The radial (a) and axial (b) PWR benchmark core configuration [22].

Table 8. Operational data for the A1, A2, B1 and B2 benchmark cores.

Case name	Core condition	Number of ejected CR	Initial position of CR (in steps) / Number	
			Ejected	Not ejected
A1	HZP	1 (central)	0 /1	228 / 40
A2	HFP	1 (central)	100 / 1	200 / 40
B1	HZP	4 (peripheral)	0 / 4	0 / 5 228 / 32
B2	HFP	4 (peripheral)	150 / 4	150 / 1 228 / 36

Table 9 shows steady state and transient results of case A1 and B1 at HZP condition, and case A2 and B2 at HFP condition. All calculation results of NODAL3 are compared to the reference solutions of PANTHER which were published in 1993 (PANTHER-1993) [32] and

revised in 1997 (PANTHER 1997) [33].

The NODAL3 steady state results in term of the critical boron concentration show the maximum deviations of 0.85% and 0.42% compared with the published and revised PANTHER solutions, respectively. It is worthily noted that the deviation of 0.85% is equivalent to only 10.1 ppm of boron concentration difference. For the critical boron concentration, the results of NODAL3 code are in a very good agreement with the revised reference results. Therefore, the feedback model which handles the cross sections by their derivatives and boron concentrations is correctly implemented in the code.

The behavior of reactor power and average Doppler temperature are shown in Figs. 2-5. If the PANTHER-1993 is used as the reference solution, the maximum deviation of 12% (using AM method) occurs in the calculated power peak of Case B1, while, if the PANTHER-1997 is used, the maximum deviation of 26% occurs in the calculated time of power peak of Case B2. The deviation of 26% is equivalent to Δt = 26 ms difference, i.e. the power peak of NODAL3 occurs nearly 26 ms later. The deviation of the calculated power peak of Case B1 increased to 18% if it is compared to the PANTHER-1997 result. On the other hand, compared with both references, the deviation of calculated final power (at 5 s) shows good agreement by the maximum of 3.6%. Since there is no systematic difference, the numerical methods for treating the coupled neutronics thermal-hydraulics in the NODAL3 code are considered correct. Probably this benchmark cases are sensitive, especially, concerning the control rod reactivity. Therefore, sensitivity analysis needs to be done in the future to know clearly the cause of the deviations.

The maximum deviations of the fuel temperature parameters obtained by NODAL3 are lower compared to the final power parameters, since they are only 0.5% (ΔT=1.1 ^{o}C) and 3.1% (ΔT=20.8 ^{o}C) for the final average Doppler temperature and the maximum fuel temperature, respectively. For the final coolant outlet temperature, the maximum deviation of NODAL3 is 5.3% or equivalent to ΔT = 16 ^{o}C. Moreover, Table 9 and Figs. 2-6 show that the AM and QSM methods are very similar for all cases and all transient parameters with the maximum deviations of 4.1%.

A comparison with other codes that have been validated for the same benchmark, namely ANCK [34] and DYN3D/R [35] codes, has been carried out, although the results are not shown here. It should be noted that the maximum deviation (%) for the DYN3D/R code was compared only to the PANTHER-1993, while for the ANCK code was compared to the reference PANTHER-1997. It is confirmed that the maximum deviations of NODAL3 code are in the same order compared to ANCK and DYN3D/R codes.

V. CONCLUSIONS AND FUTURE WORKS

A coupled neutronics thermal-hydraulics code, NODAL3, based on the few-group nodal neutron diffusion theory in 3-dimensional Cartesian geometry using the polynomial nodal method, has been developed and verified against the NEACRP LWR Core Transient Benchmark. The results of NODAL3 code show very good agreement with the PHANTHER reference solutions and other validated codes. As the future works, sensitivity analyses are planned for

assessing the accuracy of the code by changing the number of radial/axial nodes, number of radial mesh for the pellet and clad regions, maximum time steps etc. In the present version of NODAL3 code, only a simple thermal-hydraulics single channel PWR model is implemented. Further verification and improvement of the model are expected to be conducted in the future.

Table 9. The calculation results of NODAL3 code for NEACRP 3-D LWR benchmark problems.

Parameter	Case/Core Condition			
	A1/HZP	A2/HFP	B1/HZP	B2/HFP
Critical boron concentration, ppm				
PANTHER(1993)	567.7	1160.6	1254.6	1189.4
PANTHER(1997)	561.2	1156.6	1248.0	1183.8
NODAL3 (adiabatic)	563.0	1151.7	1253.0	1179.3
NODAL3 (quasistatic)	563.0	1151.7	1253.0	1179.3
Time of power peak, s				
PANTHER(1993)	0.560	0.100	0.517	0.120
PANTHER(1997)	0.538	0.095	0.523	0.100
NODAL3 (adiabatic)	0.566	0.099	0.501	0.126
NODAL3 (quasistatic)	0.579	0.100	0.507	0.121
Power peak				
PANTHER(1993)	1.18	1.080	2.44	1.063
PANTHER(1997)	1.27	1.083	2.32	1.064
NODAL3 (adiabatic)	1.17	1.076	2.73	1.055
NODAL3 (quasistatic)	1.15	1.076	2.67	1.055
Final power (at 5 s)				
PANTHER(1993)	0.196	1.035	0.32	1.038
PANTHER(1997)	0.197	1.036	0.32	1.039
NODAL3 (adiabatic)	0.190	1.032	0.31	1.033
NODAL3 (quasistatic)	0.190	1.032	0.31	1.033
Final average Doppler temperature (at 5 s), ^{o}C				
PANTHER(1993)	324.30	554.60	349.9	552.0
PANTHER(1997)	324.90	555.20	350.0	552.4
NODAL3 (adiabatic)	323.26	555.71	349.1	552.2
NODAL3 (quasistatic)	323.17	555.83	348.9	552.5
Maximum fuel temperature (at 5 s), ^{o}C				
PANTHER(1993)	673.3	1691.8	559.8	1558.1
PANTHER(1997)	679.3	1679.6	559.7	1576.1
NODAL3 (adiabatic)	659.6	1699.1	554.9	1598.0
NODAL3 (quasistatic)	658.5	1699.0	554.1	1598.0
Final coolant outlet temperature (at 5 s), ^{o}C				
PANTHER(1993)	293.1	324.6	297.6	324.5
PANTHER(1997)	293.2	324.9	297.7	324.8
NODAL3 (adiabatic)	308.7	335.1	303.1	334.6
NODAL3 (quasistatic)	308.7	335.1	303.0	334.6

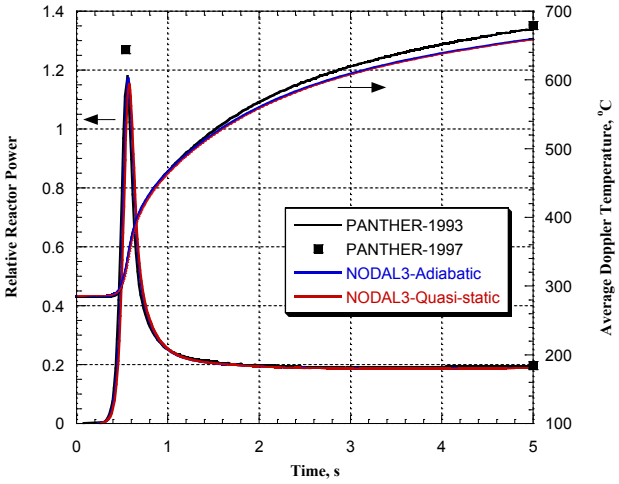

Figure 6: Comparison between NODAL3 and references results for the Case A1.

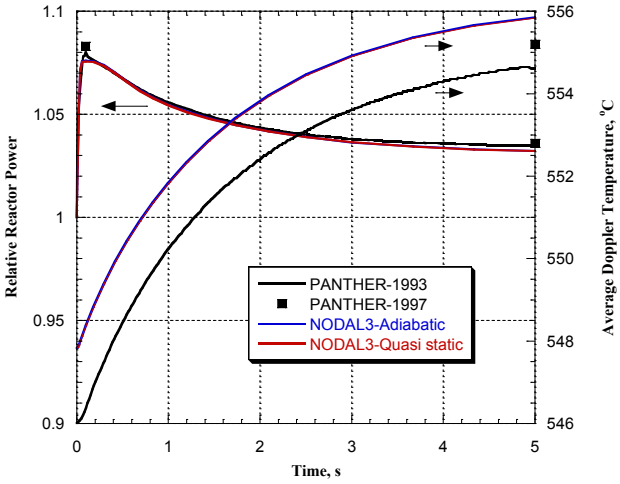

Figure 7: Comparison between NODAL3 and references results for the Case A2.

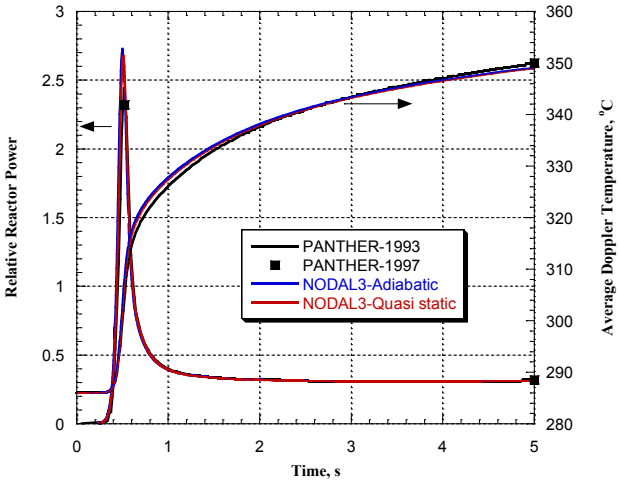

Figure 8: Comparison between NODAL3 and references results for the Case B1.

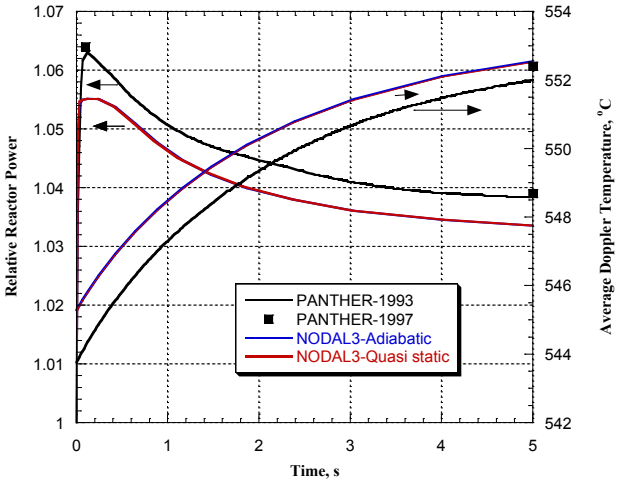

Figure 9: Comparison between NODAL3 and references results for the Case B2.

ACKNOWLEDGMENTS

This work has been partially supported by the Finance Ministry and Research & Technology Ministry of Indonesia for fiscal years of 2010-2012.

REFERENCES

[1] International Energy Agency, *World Energy Outlook 2010*. OECD/IEA, Paris, France, 2010.

[2] Presidential Decree of Republic of Indonesia No. 5 Year 2006 on National Energy Policy.

[3] P.H. Liem, "Development and verification of BATAN's standard two-dimensional multigroup neutron diffusion code (BATAN-2DIFF)," *Atom Indonesia*, vol. 20, no. 2, pp. 1-19, 1994.

[4] P.H. Liem, "Development of BATAN's standard 3-D multigroup diffusion code (BATAN-3DIFF)", *Proc. 5-th Workshop of Computation in Nuclear Science and Technology*, Batan, Jakarta, Indonesia, 1995.

[5] P.H. Liem, "BATAN-ADJOINT-2D: BATAN's standard code for calculations of integral kinetic parameters of nuclear reactors," *Atom Indonesia*, vol. 21, no. 2, pp. 1-18, 1995.

[6] P.H. Liem, "Development and verification of BATAN's standard diffusion code modules for treating triangular mesh geometry," *Atom Indonesia*, vol. 24, no. 2, pp. 75-93, 1998.

[7] T.M. Sembiring and P.H. Liem, "Validation of BATAN's standard diffusion codes on IAEA benchmark static calculations," *Atom Indonesia*, vol. 23, no. 2, pp. 73-91, 1997.

[8] P.H. Liem and T.M.Sembiring, "Validation of BATAN's standard neutron diffusion codes for control rod worth analysis," *Atom Indonesia*, vol. 23, no. 2, pp. 55-72, 1997.

[9] Zuhair, T.M. Sembiring and P.H. Liem, "BATAN-2DIFF and-3DIFF diffusion codes validation on Kyoto University Critical Assembly (KUCA)," *Atom Indonesia*, vol. 24, no. 1, pp. 15-32, 1998.

[10] P.H. Liem, "Validation of BATAN standard 3-D diffusion code, BATAN-3DIFF, on first core of RSG-GAS," *Atom Indonesia*, vol. 25, no. 1, pp. 47-64, 1999.

[11] T.M. Sembiring and P.H. Liem, "Validation of BATAN-3DIFF code on 3-D model of the IAEA 10 MWth benchmark core for partially-inserted control rods," *Atom Indonesia*, vol. 25, no. 2, pp. 91-100, 1999.

[12] P.H. Liem, "BATAN-FUEL: A general in-core fuel management code," *Atom Indonesia*, vol. 22, no. 2, pp. 67-80, 1996.

[13] P.H. Liem, "Development of an in-core fuel management code for searching equilibrium core in 2-D reactor geometry (BATAN-EQUIL-2D)," *Atom Indonesia*, vol. 23, no. 1, pp. 1-19, 1997.

[14] P.H. Liem, B. Arbie, T.M. Sembiring, Prayoto and R. Nabbi, "Fuel management strategy for the new equilibrium silicide core design of RSG GAS (MPR-30)," *Nuclear Engineering and Design*, 180, pp. 207–219, 1998.

[15] T.M. Sembiring, Tukiran, S. Pinem, Febrianto, "Neutronic design of mixed oxide-silicide cores for the core conversion of RSG-GAS reactor," *Atom Indonesia*, vol. 27, no. 2, pp. 85-101, 2001.

[16] S. Pinem and T.M. Sembiring**, "**Application of neutronics modelling on the transient simulation of RSG-GAS reactor," *Proc. of the International Conference on Mathematics and Natural Science*, ITB, Bandung, Indonesia, pp 1056 – 1059**,** 2006.

[17] S. Pinem and T.M. Sembiring**,** "Transient analysis of RSG-GAS reactor core for coolant flow reduction using MTR-DYN code," *Journal of Nuclear Reactor Technology Tri Dasa Mega*, vol. 11, no. 3, pp. 153 – 161, 2009.

[18] Presidential Regulation of Republic of Indonesia No. 5 Year 2010 on National Medium-Term Development Plan 2010-2014.

[19] R.J.J. Stamm'ler and M. Abbate, *Reactor Physics in Nuclear Design*. Academic Press, London, England, 1983.
[20] H. Finnemann, F. Bennewitz and M.R. Wagner, "Interface current techniques for multidimensional reactor calculations," Atomkernenergie, vol. 30, no.2, p.123-128, 1977.
[21] T.M. Sembiring and S. Pinem, "The validation of the NODAL3 code for static cases of the PWR benchmark core," *Journal of Nuclear Science and Technology Ganendra*, vol. 15, no.2, pp. 82-92, 2012.
[22] H. Finnemann and A. Galati, "NEACRP 3-D LWR core transient benchmark. Final specifications," NEACRP-L-335 (Revision 1), 1992.
[23] R. Fraikin, "NEA-NSC 3-D/1-D PWR Core Transient Benchmark Uncontrolled Withdrawal of Control Rods at Zero Power. Final specifications," NEA/NSC(93)9, 1993.
[24] P.J. Turinsky, "NESTLE: A few-group neutron diffusion equation solver utilizing the nodal expansion method for eigenvalue, adjoint, fix source steady-state and transient problems," Idaho National engineering Laboratory, EGG-NRE-11406, 1994.
[25] "NODAL3: A Nodal Neutron Diffusion Code, version 2," User's Guide, 2010.
[26] K.O. Ott and R.J. Neuhold, *Introductory Nuclear Reactor Dynamic*, American Nuclear Society, Illinois, USA, 1985.
[27] E.Z. MULLER and E.J. WEISS, *Ann. Nucl. Energy*, 18, (1991) 535-544
[28] R.R. LEE et al., *Argonne Code Centre: Benchmark Problem Book*, Report No.: ANL-7416, Supp. 2, ID.11-A2, Argonne National Laboratory (US), (1977) 277-466
[29] https://engineering.purdue.edu/PARCS/Code/TestSuite/CalculationMode/StandAloneMode/Eigenvalue/IAEA3DPWR/Output/iaea3d.out (2012)
[30] I. Ariani and D. Kastanya, "Evaluation of the IAEA-3D PWR Benchmark Problem Using NESTLE Code," *Prosiding Lokakarya Komputasi Dalam Sains dan Teknologi Nuklir ke-15*, PPIN-BATAN, (2005) pp. 20-25.
[31] S. Pinem, T.M. Sembiring and P.H. Liem, "The Verification of Coupled Neutronics Thermal-Hydraulics Code NODAL3 in the PWR Rod Ejection Benchmark," *Science and Technology of Nuclear Installations*, 2014.
[32] H. Finnemann, et al., "Results of LWR core transient benchmark," NEA/NSC/DOC(93) 25, 1993.
[33] M.P. Knight and P. Bryce, "Derivation of a Refined PANTHER Solution to the NEACRP PWR Rod Ejection Transients," 1997.
[34] S. Aoki, et al., "The verification of 3-dimensional nodal kinetics code ANCK using transient benchmark problems," *Journal of Nuclear Science and Technology*, vol. 44, no. 6, pp. 862–868, 2007.
[35] U. Grundmann and U. Rohde, "Verification of the code DYN3D/R with the help of international benchmarks," FZR-195, Research Center Rossendorf Inc., Dresden, Germany, 1997.